

An Improved Energy Management Strategy For A Hybrid Fuel Cell/Battery Passenger Vessel

Ameen M. Bassam^{a,b,*}, Alexander B. Phillips^c, Stephen R. Turnock^a, Philip A. Wilson^a

^aFluid Structure Interactions Group, University of Southampton, Boldrewood Innovation Campus, SO16 7QF, UK

^bNaval Architecture and Marine Engineering Department, Faculty of Engineering, Port Said University, Port Fouad, Egypt

^cNational Oceanography Centre, Natural Environment Research Council, UK

Abstract

The combination of a fuel cell and an energy storage system for the reduction of fuel consumption and improving the dynamics of hybrid power systems has successfully been used in transportation applications. In order to realise the benefits of hybrid fuel cell power systems, an energy management strategy is essential for distributing the required power properly between the fuel cell and the energy storage system. For a hybrid fuel cell/battery passenger vessel, an improvement to the classical proportional-integral (PI) controller based energy management strategy is presented. This takes fuel cell efficiency into consideration as an input to maintain higher efficiency of fuel cell and reduce stresses on it and hence reduce its fuel consumption.

A 25.5 m long passenger vessel is used and its propulsion system is modelled in MATLAB/Simulink environment using the SimPowerSystems toolbox. The performance of the proposed PI energy management strategy is compared to original PI, equivalent fuel consumption minimization strategy (ECMS), and state-based energy management strategies in terms of consumed energy, battery state of charge, fuel cell efficiency, hydrogen consumption, and the stresses seen by each power source of the hybrid system taking into consideration a daily operation of 8 hours. Results indicate that a daily hydrogen saving of 3.5%, 1.7%, and 1.4% compared to the ECMS, state-based, and the original PI strategies respectively can be achieved by adopting the proposed PI strategy in addition to lower stress on the fuel cell.

Keywords: Energy Management Strategy, Hybrid Power System, Fuel Cell, PEMFC, PI Controller.

1. Introduction

Much research in recent years has focused on using fuel cells in hybrid electric propulsion systems for transportation applications in order to reduce its negative environmental impacts [1]. For marine applications, hybrid electric propulsion is one of the energy efficiency design index (EEDI) related measures suggested by the International Maritime Organization (IMO) to control ship emissions [2]. Using fuel cells as a main source of power increases the potential of hybrid electric propulsion systems to reduce energy demand and pollution [3, 4].

Among the various fuel cell technologies available, proton exchange membrane fuel cell (PEMFC) is considered the most promising because of its solid electrolyte, high efficiency even at low loads, low operating temperature, quick start-up, high power density, low noise, and zero emission [5, 6]. However, PEMFC has a time-delayed response, therefore an energy storage system is normally used with the fuel cell in a hybrid power system [7, 8]. Hybridizing fuel cells with an energy storage system can improve the dynamics and efficiency of the power system,

lower its size, and reduce its cost. Moreover, since part of the load will be provided by the energy storage system, fuel cell performance can be optimized specially during rapid load changes [8, 9]. This optimization is achieved through an energy management strategy (EMS).

For hybrid fuel cell propulsion systems, the proper split of the required power between the fuel cell system and the energy storage system is a challenging problem which requires the design of an EMS. This EMS will control the dynamic behaviour of the hybrid power system components which affects the system efficiency, fuel consumption and lifetime. Therefore, developing a suitable EMS for hybrid fuel cell propulsion system has been a very important research topic [7, 8, 10]. The objectives of an EMS include reducing hydrogen consumption, increasing the fuel cell efficiency, reducing the size and weight of the power system, reducing the operation cost, reducing the stress on the power system components to prolong its working lifetime [11, 12, 13]. EMS objectives also include reducing emissions, maintaining the battery state of charge (SOC) or the bus voltage at a certain level [10, 14].

Most of the work reported in the literature on EMS tends to focus on the automotive industry applications; however, several studies have been made on developing EMS for marine applications. A state-based EMS has been

*Corresponding author

Email address: ab2e12@soton.ac.uk (Ameen M. Bassam)

47 developed in [15] for a passenger vessel equipped with a
 48 fuel cell/battery hybrid power system with the main objec-
 49 tive of maximizing the system efficiency. For the same ves-
 50 sel, a fuel cell/battery/ultra-capacitor hybrid power sys-
 51 tem with a fuzzy logic EMS has been proposed in [16] to
 52 further enhance the performance of the hybrid system. A
 53 hybrid fuel cell/battery system was developed for a 20 m
 54 long tourist boat in Korea with a total power of about 90
 55 kW. The developed EMS for this boat aims to provide the
 56 required power using mainly the fuel cell system in a load-
 57 following mode and discharge the battery power whenever
 58 the required power is higher than the fuel cell system avail-
 59 able power [17]. For underwater vehicles and small ships,
 60 an EMS has been developed which requires the fuel cell to
 61 provide an average power demand, while the energy stor-
 62 age system is discharged or recharged when the required
 63 power is higher or lower the average power demand sup-
 64 plied by the fuel cell [12, 18].

65 The aim of this work is to improve the classical
 66 proportional-integral (PI) controller based EMS for a
 67 hybrid fuel cell/battery passenger vessel. This improve-
 68 ment includes taking fuel cell efficiency into consideration
 69 as an input to the PI EMS in order to maintain high
 70 efficiency of the fuel cell and better performance which
 71 helps in reducing its fuel consumption, reducing stress on
 72 it, reducing its maintenance and replacement costs, and
 73 extending its lifetime. The performance of the proposed
 74 PI EMS is compared with that from three alternative
 75 strategies: the original PI EMS, the state-based EMS de-
 76 veloped in [15] for the same vessel and the equivalent fuel
 77 consumption minimization strategy (ECMS) which gives
 78 a near-optimal performance. For a full mission profile of 8
 79 hours, the performance comparison is carried out in terms
 80 of the consumed energy, battery SOC, fuel cell efficiency
 81 and hydrogen consumption. The criteria for performance
 82 comparison includes as well the stress on each power
 83 source measured using Haar wavelet transform. These
 84 stresses impact on the lifetime of the hybrid power system
 85 components.

86 The paper is organized as follows. Section 2 describes
 87 the examined vessel and its propulsion system. Section
 88 3 outlines the implementation of the four energy manage-
 89 ment strategies. Section 4 shows the simulation results and
 90 validation. Finally, the work conclusions are presented in
 91 Section 5.

92 2. Vessel & Voyage Description

93 This study uses the world’s first hydrogen fuel cell pas-
 94 senger vessel ‘FCS Alsterwasser’ as a case study. This ves-
 95 sel was developed as part of the ZEMSHIPS project funded
 96 by the EU-Life program [19]. A hydrogen filling station
 97 has been built by Linde Group as a part of this project.
 98 FCS Alsterwasser operates around Hamburg, Germany on
 99 Lake Alster, HafenCity, the River Elbe and the inner city
 100 waterways for round and charter trips [19]. This vessel has

101 been classified by the Germanischer Lloyd and its main
 102 particulars are shown in Table 1.

Table 1: Specifications of the FCS Alsterwasser passenger vessel

Capacity	100 passengers
Length	25.5 m
Breadth	5.36 m
Depth	2.65 m
Draft	1.33 m
Displacement	72 tonnes
Top speed	8 kn
Powering	2 PEMFC of 48 kW each 360 Ah/560 V lead-gel battery

103 FCS Alsterwasser is equipped with two PEMFC with
 104 a peak power of 48 kW each, which have proven to be an
 105 extremely reliable energy source connected to the DC bus
 106 using a DC-DC converter to control the voltage. A 360 Ah
 107 battery is also connected directly to the DC bus to power a
 108 100 kW electric motor as shown in Figure 1. The vessel is
 109 also equipped with twelve hydrogen tanks at a pressure of
 110 350 bar and a hydrogen weight of 50 kg which is sufficient
 111 for two or three days of operation without refuelling [17].
 112 The required time for filling the hydrogen tanks is about
 113 twelve minutes [20].

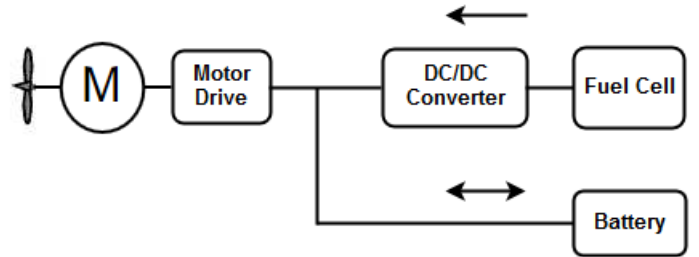


Figure 1: Configuration of the vessel fuel cell/battery hybrid propul-
 sion system

114 An extract of the power requirements for a typical voy-
 115 age on the Alster, Hamburg, Germany has been measured
 116 and published in [19, 15]. This power requirement includes
 117 propulsion and auxiliary power. The data measured from
 118 [15] shown in Figure 2 starts with a cruising time of about
 119 90 seconds, the vessel then enters a docking phase lasting
 120 45 seconds. The vessel is alongside for 25 seconds. Finally
 121 the vessel starts to sail again and reaches its cruising speed
 122 after an acceleration time of about 35 seconds, giving 300
 123 seconds total time for the manoeuvre.

124 Based on the typical power consumption shown in Fig-
 125 ure 2, the power consumption of a complete voyage from
 126 Finkenwerder to Landungsbrücken has been extrapolated
 127 as shown in Figure 3. Duration of the full journey is about
 128 1 hour as shown in Table 2 with 4 stops between the two
 129 destinations as shown in Figure 4 [21].

130 In order to cover a daily vessel operation of 8 hours,
 131 the developed load power requirement shown in Figure 3

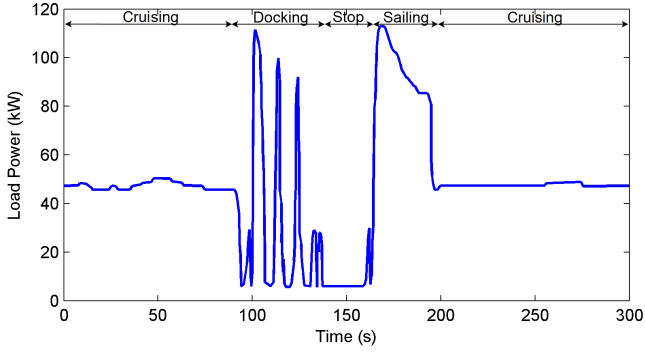


Figure 2: Part of the real typical load characteristics on the Alster

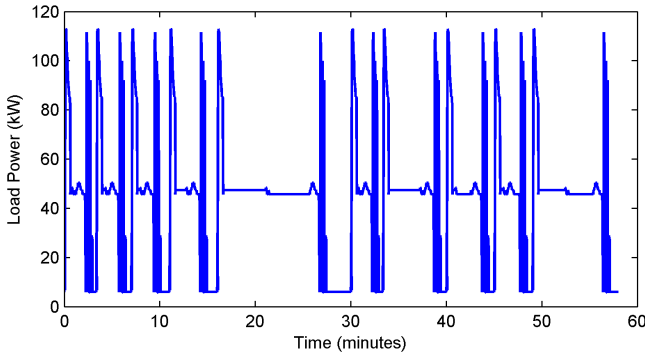


Figure 3: Developed power requirement of a real full voyage between Finkenwerder and Landungsbrücken

has been repeated for 8 times in order to be used as an input to the simulation of the EMS as will be described in the following sections.

3. Energy Management Strategy

3.1. State-based EMS

State-based control is one of the deterministic rule-based methods used to control each component of the hybrid system for different transportation applications. This kind of strategy can have many operating states to decide the operating points of the fuel cell and battery systems according to the required power and the battery SOC taking into consideration the operational limits of the hybrid system components [22, 23].

For the same vessel 'FCS Alsterwasser', a state-based EMS was developed in [15] to determine the proper split

Table 2: Finkenwerder - Landungsbrücken time table [21]

Landungsbrücken	19.15	Finkenwerder	19.45
Altona	19.18	Bubendey-Ufer	19.48
Dockland	19.22	Neumuhlen	19.55
Neumuhlen	19.26	Dockland	20.00
Bubendey-Ufer	19.31	Altona	20.04
Finkenwerder	19.43	Landungsbrücken	20.13

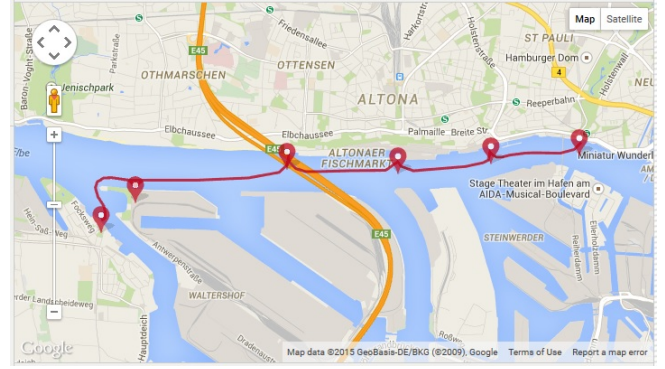


Figure 4: The examined vessel route [21]

of the required power between the components of the hybrid fuel cell/battery system with an objective of maximizing the system efficiency. This strategy consists of 11 states for 11 possible cases of combination between battery SOC, required load power (P_{load}), fuel cell minimum power (P_{FCmin}), optimum fuel cell power (P_{FCopt}), maximum fuel cell power (P_{FCmax}), battery optimum discharge power (P_{optdis}), battery optimum charge power ($P_{optchar}$) and battery optimum power (P_{BATopt}) as shown in Table 3.

The value used for the battery optimum charge is equal to optimum discharge power with 30% battery capacity while battery optimum power equates to 20% battery capacity as suggested in [15]. Fuel cell minimum, optimum, and maximum power values are selected based on the current and voltage limits of the fuel cell in order to maximize the system efficiency which is the main objective of this EMS. The main inputs of this EMS are the required load power and the battery SOC which are used to decide the fuel cell power. Then, the difference between the required load power and the fuel cell power is used to charge or discharge the battery.

In this EMS, as can be seen in Table 3, fuel cells operate at minimum power when the battery SOC is normal or high and the required load power is not too high as in states 1, 2, and 5. During high required load power or low battery SOC, fuel cells operate at its maximum power as in states 4, 9 and 11 to provide the required load power and charge the battery. Meanwhile fuel cells are regulated to follow the load power in states 3, 6, 8 and 10 and it works at its optimum power value in state 7 only.

3.2. Original & Proposed PI EMS

Recently, EMS based on classical PI and PID controllers have been proposed due to their simplicity, these can be easily tuned for the examined mission profile. The main goal of original PI EMS is to maintain the battery SOC at its nominal value in order to reduce the stress on it and extend its lifetime [9, 10]. In the original PI EMS, the current battery SOC is compared to a reference value of battery SOC (SOC_{Ref}) to control the battery power or

Table 3: Summary of a state-based EMS [15]

Battery SOC	State	Load Power	Fuel cell reference power
SOC > 80%	1	$P_{load} \leq P_{FCmin}$	P_{FCmin}
	2	$P_{load} \leq P_{FCmin} + P_{optdis}$	P_{FCmin}
	3	$P_{load} \leq P_{FCmax} + P_{optdis}$	$P_{FC} = P_{load} - P_{optdis}$
	4	$P_{FCmax} + P_{optdis} < P_{load}$	P_{FCmax}
$50\% \leq SOC \leq 80\%$	5	$P_{load} \leq P_{FCmin}$	P_{FCmin}
	6	$P_{load} \leq P_{FCopt} - P_{BATopt}$	P_{load}
	7	$P_{load} \leq P_{FCopt} + P_{BATopt}$	P_{FCopt}
	8	$P_{load} \leq P_{FCmax}$	P_{load}
	9	$P_{load} > P_{FCmax}$	P_{FCmax}
SOC < 50%	10	$P_{load} \leq P_{FCmax} - P_{optchar}$	$P_{load} + P_{optchar}$
	11	$P_{load} > P_{FCmax} - P_{optchar}$	P_{FCmax}

187 current using PI controller as shown in Figure 5. This battery
 188 power is subtracted from the load power to calculate
 189 the fuel cell power. Then, the battery and fuel cell power
 190 are divided by the voltage to calculate the current drained
 191 from the fuel cell and battery. By discharging/charging
 192 the battery, battery SOC will change and will be fed back
 193 to the EMS block to close the loop of the PI controller.

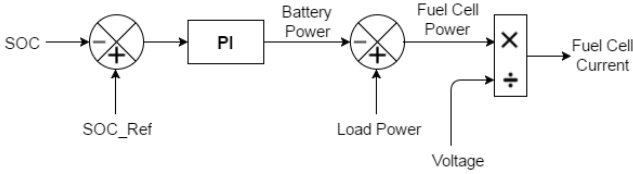


Figure 5: Original PI control energy management strategy scheme [9]

194 The inputs of this EMS are the battery SOC and the
 195 required load power with an ultimate goal of maintaining
 196 the battery SOC around its reference value which makes
 197 the fuel cell follow the required load power or operate at its
 198 maximum power when the current battery SOC drops below
 199 its reference value. This effects the fuel cell efficiency,
 200 hydrogen consumption and lifetime. Therefore, a proposed
 201 PI EMS is developed in this paper that takes fuel cell effi-
 202 ciency into account as an input to the EMS. By avoiding
 203 the operation of fuel cells in a poor efficiency region, its
 204 fuel consumption can be reduced. Furthermore, its opera-
 205 tional stresses can be lowered that allows the reduction of
 206 fuel cell maintenance cost and extending its lifetime.

207 In the proposed PI EMS, fuel cell efficiency (FC_Eff)
 208 is taken into consideration by comparing it to a reference
 209 value (FC_Eff_Ref) in order to control the fuel cell current
 210 which is removed from the required load current to obtain
 211 the battery current. Then, the battery current is updated
 212 according to the difference between the current battery
 213 SOC and its reference value as shown in Figure 6 ensuring
 214 that the power requirement is completely satisfied. By
 215 consuming power from the battery and fuel cell, battery
 216 SOC and fuel cell efficiency will change and fed back to
 the EMS to close the loops of the PI controllers.

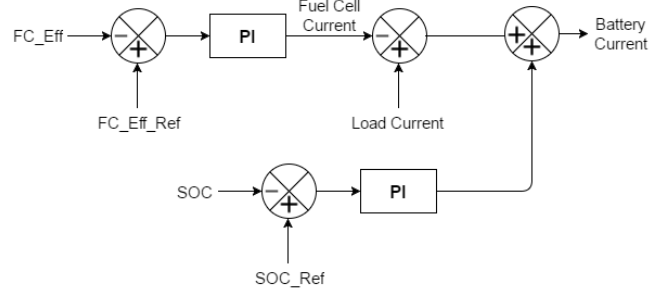


Figure 6: Proposed PI control energy management strategy scheme

218 PI controllers can be reliably used for the proposed PI
 219 EMS, since fuel cell efficiency is linear with the fuel cell
 220 current for approximately 80% of load currents after an
 221 initial non-linearity region at low loads as shown in Fig-
 222 ure 15 which can be neglected [24]. Moreover, using fuel
 223 cell efficiency as an input allows the fuel cell to operate
 224 more at higher efficiency which means reduced hydrogen
 225 consumption, less stress and longer lifetime. Moreover,
 226 the proposed PI EMS maintains the required battery SOC
 227 which is the main objective of the original PI EMS. The
 228 gains of the PI controllers of the original and the proposed
 229 PI strategies are manually tuned for the examined driv-
 230 ing cycle with the help of the MATLAB control system
 231 toolbox in order to have balance between the controller
 232 performance and robustness [25].

3.3. Equivalent fuel consumption minimization strategy

234 One of the most common real-time optimization control
 235 methods is the ECMS which generates a near-optimal
 236 solution of the required power split problem. ECMS does
 237 not require a priori knowledge of the future power require-
 238 ment and its concept is to minimize the instantaneous fuel
 239 consumption of the hybrid system [9, 26]. This concept
 240 was proposed in [27] to develop an instantaneous opti-
 241 mization EMS for hybrid vehicles. The equivalent fuel
 242 consumption (C) includes the actual fuel cell hydrogen
 243 consumption (C_{FC}) as well as the equivalent consumption
 244 of the battery storage system (C_{Batt}). The optimization

245 problem to minimize the hydrogen consumption can be
 246 defined as follows:

$$P_{FCopt} = \underset{C}{\operatorname{argmin}} P_{FCopt} = \underset{C}{\operatorname{argmin}} (C_{FC} + \alpha \cdot C_{Batt}) \quad (1)$$

247 where (α) is a penalty coefficient which is used to accom-
 248 plish the charge-sustaining operation of the battery. It is
 249 calculated as a function of battery SOC limits as follows:

$$\alpha = 1 - 2\mu \frac{(\operatorname{SOC} - 0.5(\operatorname{SOC}_H + \operatorname{SOC}_L))}{\operatorname{SOC}_H - \operatorname{SOC}_L} \quad (2)$$

250 where (SOC_H) and (SOC_L) are the upper and lower limit
 251 of the battery SOC respectively. Meanwhile, μ is the SOC
 252 constant which is used to reflect the characteristics of the
 253 battery charge/discharge process [28]. As shown in Figure
 254 7, based on the load power and the battery SOC, the fuel cell
 255 power is decided. This fuel cell power is subtracted from
 256 the load power to calculate the battery power. Then, fuel cell
 257 and battery powers are divided by voltage to calculate the
 258 value of current.

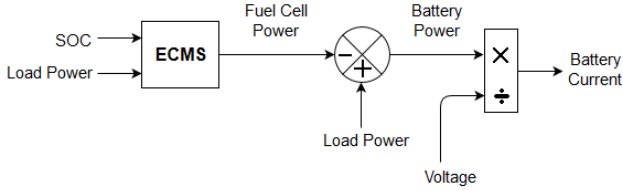


Figure 7: Equivalent fuel consumption minimization strategy scheme

259 In the next section, the components of the hybrid fuel
 260 cell/battery system of the examined passenger vessel is im-
 261 plemented in MATLAB/Simulink environment using the
 262 SimPowerSystems (SPS) toolbox. Also, the proposed PI
 263 EMS is implemented in Simulink as well as the original
 264 PI, ECMS, and the original state-based EMS which was
 265 developed for the examined ship in [15] to compare its per-
 266 formance in terms of the consumed energy, battery state of
 267 charge (SOC), fuel cell efficiency and hydrogen consump-
 268 tion.

269 4. Simulation Implementation and Results

270 The vessel fuel cell/battery hybrid system illustrated in
 271 Figure 1 is modelled mathematically in MATLAB/Simulink
 272 environment in order to study and understand the behav-
 273 iour of different energy management strategies which al-
 274 lows the design of the EMS effectively. As shown in
 275 Figure 8, the EMS subsystem converts the load required
 276 power into current and splits it between the fuel cell and
 277 the battery subsystems according to the used EMS. The
 278 modelling approach of each subsystem is described in this
 279 section.

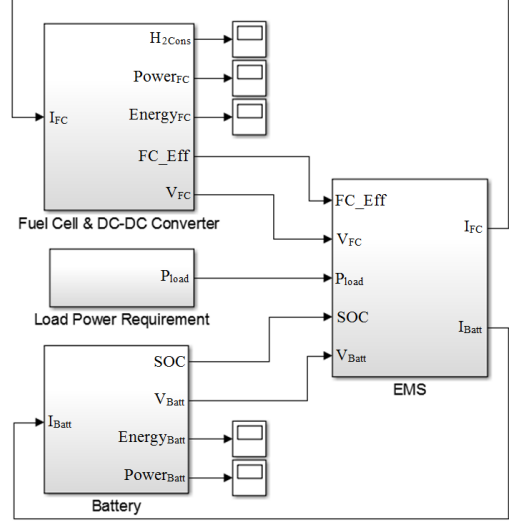


Figure 8: Hybrid fuel cell/battery power system in Simulink/MATLAB environment

4.1. Fuel cell & DC-DC converter subsystem

4.1.1. Fuel cell

280 Due to its advantages, PEMFC has been used and
 281 studied for different applications including portable, trans-
 282 portation and stationery applications. Modelling of
 283 PEMFC has attracted attention and many performance
 284 models of PEMFC have been developed. A generic model
 285 of a PEMFC developed and validated in [29] is selected
 286 in this study. This model is implemented in Simulink as
 287 shown in Figure 9 and integrated in SPS library of elec-
 288 trical power systems as a generic hydrogen fuel cell stack
 289 model.
 290
 291

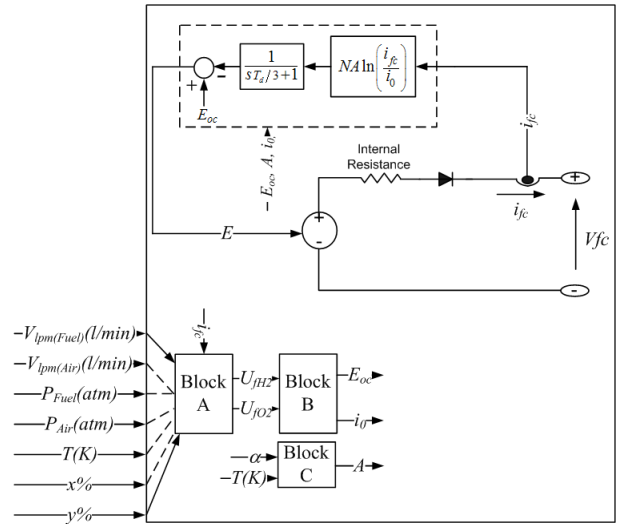


Figure 9: Fuel cell model in Simulink/MATLAB environment adapted from [30]

292 The main parameters of this model can be obtained
 293 from the fuel cell datasheet or from its polarization curve
 294 test which makes this model easy to use. This model can

295 represent both steady-state and dynamic performance of
 296 PEMFC taking fuel cell response time into consideration.
 297 Moreover, this model considers the features of electrical
 298 and chemical models. This model has been validated with
 299 experimental data as well as datasheet performance data
 300 with an error of $\pm 1\%$. More details on this model can
 301 be found in [29]. The hydrogen consumption of PEMFC
 302 ($H_{2\text{Cons}}$) can be calculated as follows [9]:

$$H_{2\text{Cons}} = \frac{N}{F} \int I_{\text{FCnet}}.dt \quad (3)$$

303 where (N) is the number of cells, (F) is the Faraday con-
 304 stant and (I_{FCnet}) is the net current drained from the
 305 PEMFC. Then, this hydrogen consumption is used to calcu-
 306 late the hydrogen cost and energy input to the PEMFC
 307 as follows:

$$\text{Energy}_{\text{FC}} = H_{2\text{Cons}} \times \text{HHV}_{\text{H}_2} \quad (4)$$

308 where (HHV_{H_2}) is the higher heating value of the hydrogen
 309 fed to the PEMFC.

310 4.1.2. DC-DC converter

311 The voltage of the hybrid system components varies ac-
 312 cording to the demanded current from each power source.
 313 Therefore, an electronic circuit is needed to stabilise the
 314 power source voltage while providing the required power.
 315 In order to regulate the output voltage of the PEMFC,
 316 a boost type unidirectional DC-DC converter is used be-
 317 tween the fuel cell system and the DC bus as shown in
 318 Figure 1 for the examined vessel [15]. The used converter
 319 is composed of an inductor L, a switch S and a diode D
 320 as shown in Figure 10. The net current supplied by the
 321 PEMFC into the DC bus through this DC-DC converter
 322 is readjusted according to the operating voltage ratio (k)
 323 [31] as follows:

$$\begin{aligned} k &= V_{\text{Batt}}/V_{\text{FC}} \\ I_{\text{FCnet}} &= I_{\text{FC}} \times k \end{aligned} \quad (5)$$

324 where (V_{Batt}) is the battery voltage, (V_{FC}) is the fuel cell
 325 voltage and (I_{FC}) is the required current from the fuel
 326 cell/DC-DC converter subsystem.

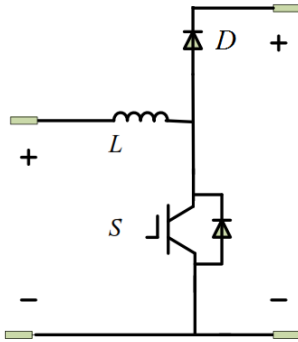


Figure 10: Electrical scheme of the fuel cell boost DC-DC converter [15]

327 For this study, a preset Simulink PEMFC model is used
 328 with a nominal power of 50 kW and maximum power of
 329 120 kW which is sufficient to provide the average load
 330 required power shown in Figure 2. The fuel cell model
 331 nominal efficiency is 55 %. It is assumed to be fed with
 332 hydrogen and air and its resistance is constant. A DC-DC
 333 converter is used to connect the fuel cell to the DC bus
 334 according to Equation 5 assuming a constant efficiency of
 335 the converter to be 95% [32].

336 4.2. Battery subsystem

337 Because batteries are considered the main energy stor-
 338 age device for transportation applications, modelling of
 339 batteries receives much attention. The SPS library in-
 340 cludes an improved easy-to-use dynamic battery model
 341 that can represent both steady state and dynamic be-
 342 haviour of the battery taking into account the response
 343 time of the battery. Therefore it is used in this study.

344 The generic battery block can simulate four types of
 345 battery which are: lead acid, lithium-ion, nickel-cadmium
 346 or nickel-metal-hydride. The battery model has been vali-
 347 dated against experimental results for the 4 different bat-
 348 tery types with a maximum error of 5% however error
 349 increase to $\pm 10\%$ when battery state of charge (SOC)
 350 decreases below 20% [33] however it is not recommended
 351 to fully discharge a battery. Figure 11 shows the equivalent
 352 circuit of the used battery model [30].

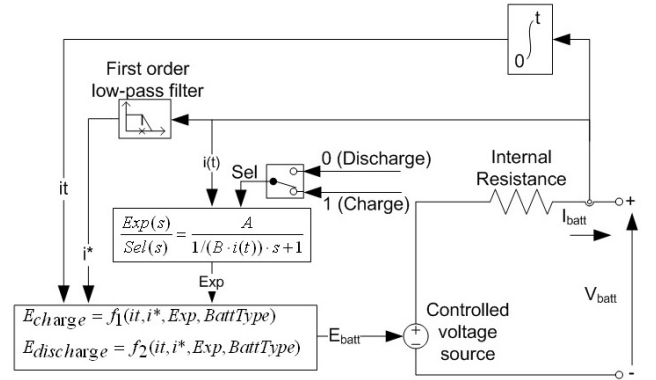


Figure 11: Battery model in Simulink/MATLAB environment adapted from [30]

353 Battery voltage (V_{Batt}) is calculated as a function of
 354 open circuit voltage (E_{batt}), internal resistance (R_{ohm}) and
 355 battery current (I_{Batt}) as follows:

$$V_{\text{Batt}} = E_{\text{batt}} - R_{\text{ohm}} \cdot I_{\text{Batt}} \quad (6)$$

356 where (E_{batt}) depends on battery type as discussed in [33].
 357 The drained power and energy from the battery can be
 358 calculated as follows:

$$\begin{aligned} \text{power}_{\text{Batt}} &= V_{\text{Batt}} \times I_{\text{Batt}} \\ \text{Energy}_{\text{Batt}} &= \int \text{power}_{\text{Batt}}.dt \end{aligned} \quad (7)$$

359 For this study, the examined vessel is equipped with a
 360 360 Ah lead-gel battery which is a lead-acid battery type
 360

361 with a voltage of 560 V [19] which is modelled using this
 362 battery model and used in this study [33].

363 4.3. EMS subsystem

364 The state-based EMS, ECMS, original PI EMS, and
 365 the proposed PI EMS are mathematically modelled and
 366 implemented in the simulation environment to make a per-
 367 formance comparison in terms of fuel cell hydrogen con-
 368 sumption and efficiency, battery SOC, total consumed en-
 369 ergy, and stresses seen by each power source. The compar-
 370 ison is made for a full driving cycle of 8 hours developed
 371 based on the available real typical load requirements shown
 372 in Figure 3.

373 The inputs of the EMS subsystem includes the required
 374 load power, fuel cell voltage and efficiency, and battery
 375 voltage and SOC. The main outputs of the EMS sub-
 376 system are the required current which will be drained of the
 377 battery and fuel cell subsystems as shown in Figure 8.
 378 Also, the EMS subsystem includes a first-order delay loop
 379 as suggested in [34] for the examined strategies in order
 380 to limit the changing rate of the required power from the
 381 fuel cell subsystem which will reduce the stress on the fuel
 382 cell and increase its lifetime.

383 Before comparing different energy management strate-
 384 gies, the results of the EMS subsystem for the state-based
 385 EMS is validated against the published results in [15] as
 386 shown in Figures 12 to 14. The hybrid fuel cell/battery
 387 system shown in Figure 1 is implemented in Simulink en-
 388 vironment using the mathematical models of PEMFC (50
 389 kW nominal power) and battery (lead-acid, 360 Ah, 560 V,
 390 65% initial SOC) as described previously. The load profile
 391 shown in Figure 2 is used as an input to the state-based
 392 EMS subsystem as suggested in [15]. The state-based EMS
 393 splits the required load power between the fuel cell in Fig-
 394 ure 12 and the battery in Figure 13 while Figure 14 shows
 395 battery SOC.

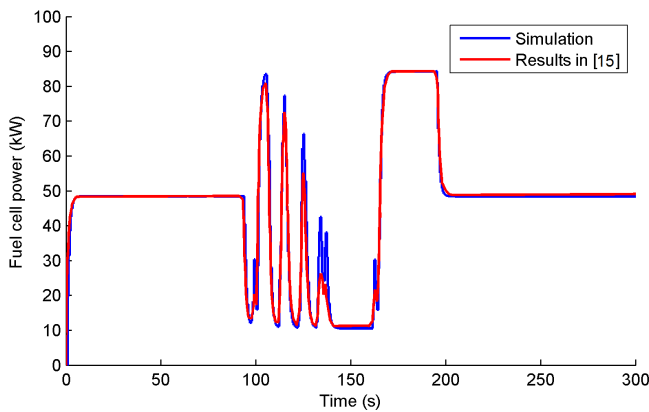


Figure 12: Validation of fuel cell power using the state-based strategy

396 Figures 12 to 14 show good agreement between the
 397 simulation results and the results published in [15]. In the
 398 following subsection, a performance comparison between
 399 the state-based EMS, ECMS, original PI EMS and the
 400 proposed PI EMS is made.

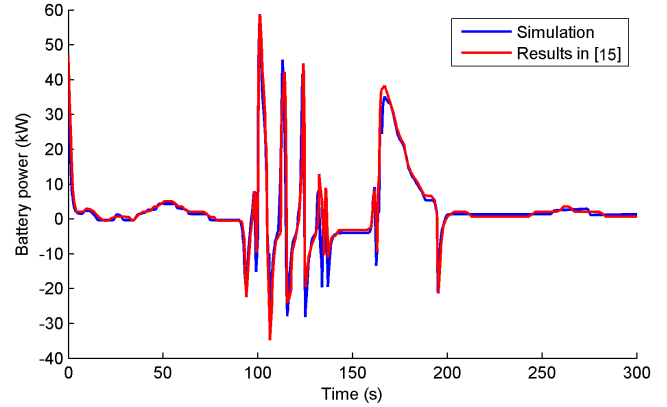


Figure 13: Validation of battery power using the state-based strategy

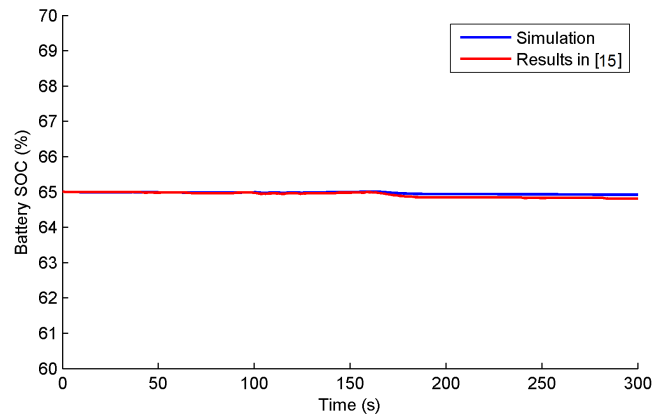


Figure 14: Validation of battery SOC using the state-based strategy

401 4.4. Results

402 In this subsection, the proposed PI EMS is compared
 403 with the original PI EMS, ECMS, and the state-based
 404 EMS which has been developed in [15] for the same ex-
 405 amined vessel. To compare different energy management
 406 strategies appropriately, the same PEMFC and battery
 407 models with the same initial conditions are used where a
 408 normal battery SOC of 65% is chosen as an initial con-
 409 dition for the examined strategies.

410 For the original and proposed PI EMS simulation, refer-
 411 ence values of the battery SOC and fuel cell efficiency
 412 should be selected carefully. The nominal efficiency of the
 413 used PEMFC model is 55% [29] which can increase at part
 414 loads [32] as shown in Figure 15. Therefore, a higher fuel
 415 cell efficiency than 55% is selected as a reference value of
 416 fuel cell efficiency for the proposed PI EMS which is 60%.

417 A nominal battery SOC of 60% is chosen as a battery
 418 SOC reference value for the original and proposed PI EMS
 419 as recommended by automotive industry designers [10].
 420 The P and I gains of the battery SOC PI controllers are
 421 50000 and 1 for the original PI EMS and 200 and 0.0001
 422 for the proposed PI EMS respectively. For the ECMS and
 423 the state-based EMS, SOC_H and SOC_L are set to 80%
 424 and 50% as suggested in [15, 35] in order to prolong the
 425 battery life. The SOC constant μ is set to 0.6 to balance

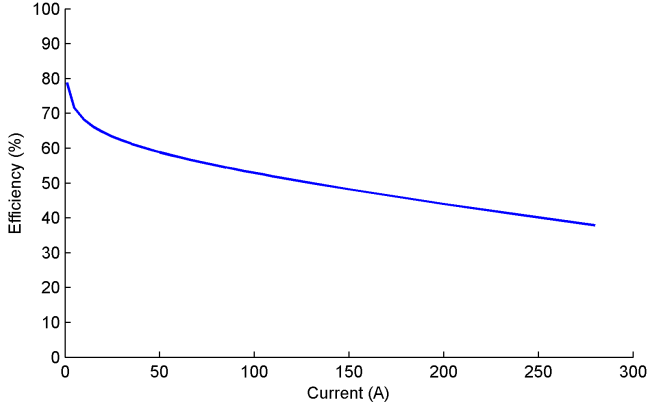


Figure 15: Fuel cell stack efficiency versus current

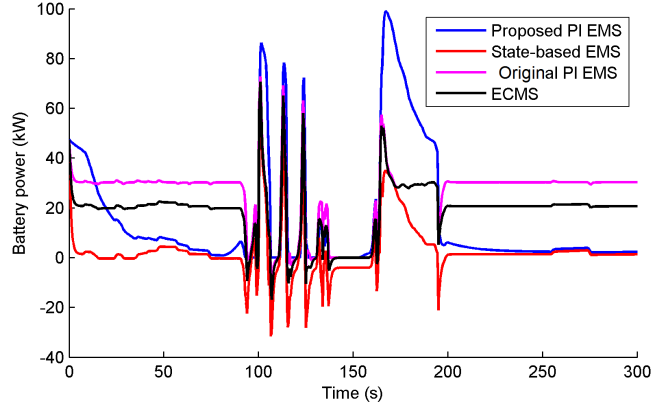


Figure 17: Comparison of battery power using different strategies

426 the battery SOC during the examined driving cycle using
 427 the ECMS as reported in [9, 26, 28].

428 In order to have a closer look on how each EMS splits
 429 the required load power between the fuel cell and the bat-
 430 tery, the same load profile shown in Figure 2 is considered.
 431 As shown in Figures 16 and 17, the state-based EMS reg-
 432 ulates the fuel cell to follow the load power because the
 433 battery SOC is normal. At high loads during docking and
 434 acceleration phases, the battery begins to work. Mean-
 435 while at low loads, the fuel cell works at its minimum
 436 power and starts to charge the battery.

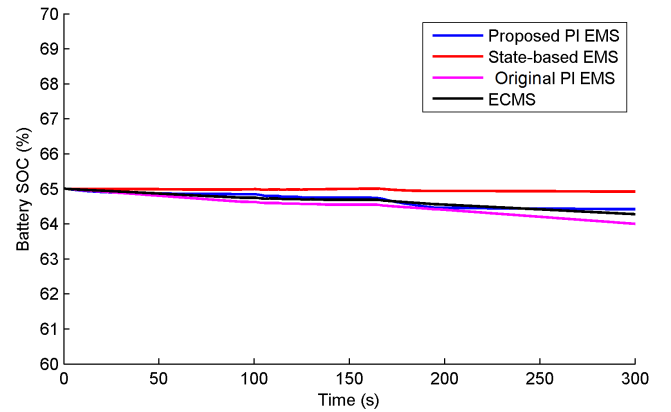


Figure 18: Comparison of battery SOC using different strategies

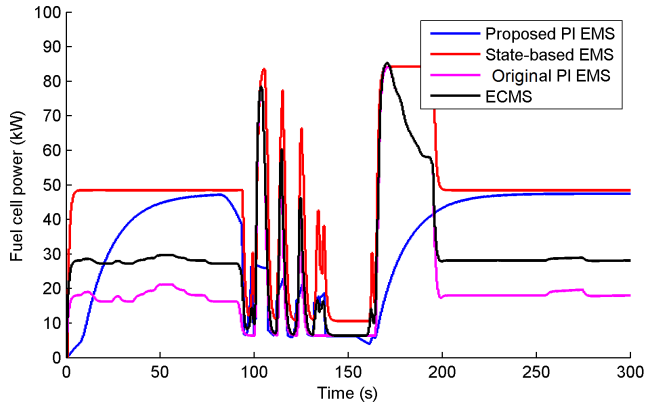


Figure 16: Comparison of fuel cell power using different strategies

437 By adopting the original PI EMS whose main objective
 438 is to maintain battery SOC at its reference value, the bat-
 439 tery starts to discharge faster to get to the battery SOC
 440 reference value as shown in Figure 18 while the fuel cell
 441 works at its minimum power and gives more power during
 442 high load phases. Because ECMS transforms the battery
 443 electrical energy consumption into an equivalent hydrogen
 444 consumption, it doesn't deplete the battery as fast as the
 445 original PI EMS.

446 In the state-based EMS and the original PI EMS, the
 447 fuel cell mostly follows the load power or works at its min-
 448 imum power which affects its efficiency and fuel consump-
 449 tion. Therefore, in the proposed PI EMS fuel cell efficiency

450 is taken into consideration as an input which results in the
 451 fuel cell spending more time at its optimum power. This
 452 also reduces the fluctuations in required load as shown in
 453 Figure 16. However, to have a better indication about the
 454 performance of each EMS and its effect on the bat-
 455 tery SOC, fuel cell efficiency and hydrogen consumption,
 456 a longer load profile should be considered.

457 For a full working cycle of 8 hours, simulation results
 458 show that, the hybrid fuel cell/battery system consumes
 459 less hydrogen using the proposed PI EMS than the ECMS
 460 by 3.4% and by 1.6% using the state-based EMS and by
 461 1.4% using the original PI EMS.

462 One reason for this saving in hydrogen consumption
 463 is taking fuel cell efficiency into consideration as an input
 464 to the EMS as proposed in this study which maintains
 465 the fuel cell efficiency around 55% or higher in the case of
 466 adopting the proposed PI EMS while fuel cell efficiency can
 467 be lower than 50% using the state-based EMS or original
 468 PI EMS as illustrated in Figure 19.

469 To compare fuel cell stack efficiency during the 8 hours
 470 driving cycle for the four different strategies, the mean,
 471 standard deviation (SD) and coefficient of variation of fuel
 472 cell efficiency are calculated. As listed in Table 4, the
 473 average value of fuel cell efficiency is similar for the four
 474 examined EMS. However, the SD and coefficient of vari-

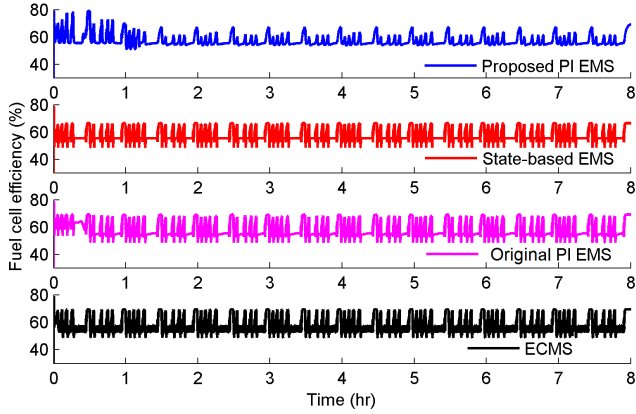


Figure 19: Fuel cell stack efficiency during the examined voyage using different strategies

475 ance of the proposed PI EMS are significantly lower by
 476 9% and 12.5% respectively compared to the state-based
 477 EMS, 25% and 30% respectively compared to the original
 478 PI EMS, and 30% and 30% respectively compared to
 479 the ECMS strategy. This means less variability and high
 480 stability of fuel cell efficiency during the examined load cycle [36] which means less stress on the fuel cell stack and
 481 results in longer lifetime and saving in hydrogen consumption.
 482
 483

Table 4: Mean, standard deviation, and coefficient of variation of fuel cell stack efficiency comparison using different strategies

	Mean (%)	SD (%)	Coefficient of variation
Proposed PI EMS	57.2	4.2	0.07
State-based EMS	57.4	4.6	0.08
Original PI EMS	57.8	5.6	0.10
ECMS	57.9	6	0.10

484 Another reason for the hydrogen consumption saving
 485 achieved by the proposed PI EMS is that the proposed PI
 486 EMS tends to use more power from the battery than the
 487 state-based EMS, the original PI EMS, and the ECMS as
 488 shown in Figure 22. The battery discharges faster in the
 489 case of the original PI EMS than the proposed PI EMS because the main objective of the original PI EMS is to maintain the battery SOC at its reference value as shown in Figure 20. However, in the case of the state-based EMS, the battery discharges more gradually which results in a higher final battery SOC of the state-based EMS. Meanwhile, ECMS maintains the battery SOC around 64% which is approximately the average value of $SOCH$ and $SOCL$. Figures 21 and 22 illustrate the fuel cell and battery power during the examined voyage using different strategies.

499 4.4.1. Sensitivity analysis

500 In order to study the effect of the selected reference
 501 value of fuel cell efficiency on the performance of the proposed
 502 PI EMS, a sensitivity analysis is performed. Differ-

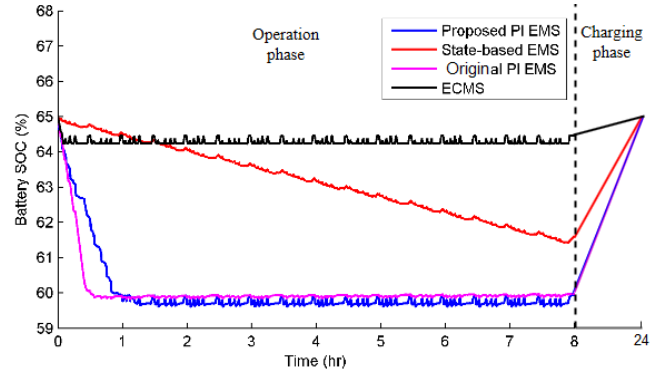


Figure 20: Battery SOC during the examined voyage using different strategies

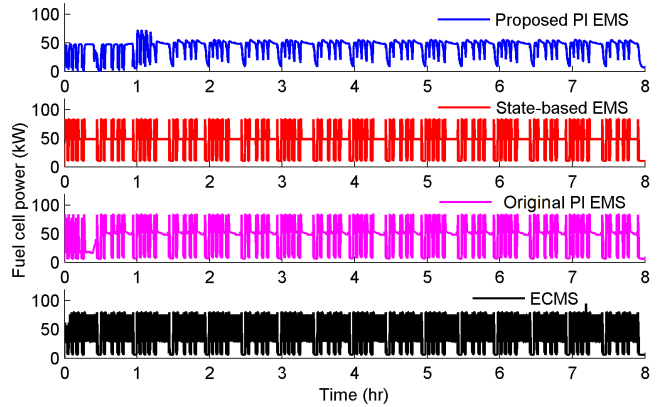


Figure 21: Fuel cell power during the examined voyage using different strategies

503 ent values of fuel cell efficiency are used as reference values
 504 for the proposed PI EMS to calculate the hydrogen consumption
 505 saving percentage using the proposed PI EMS compared to other
 506 strategies for the examined 8 hours of operation as shown in Figure 23.
 507

508 As shown in Figure 23, fuel cell efficiency reference
 509 value starts from the fuel cell stack nominal efficiency of
 510 55%. By increasing the fuel cell efficiency reference value,
 511 the hydrogen consumption saving percentage increases until
 512 65% where it starts to level off. This levelling off is expected
 513 because higher fuel cell efficiency is achieved in the low load
 514 region as shown in Figure 15 where it is difficult to operate
 515 because of the vessel required power and the fuel cell and battery
 516 operational limits. Therefore, the optimum reference value of
 517 fuel cell efficiency for the proposed PI EMS that gives the lowest
 518 hydrogen consumption is 65% for the examined full driving cycle
 519 of 8 hours. The hydrogen consumption saving percentages of the
 520 proposed PI EMS using the optimum reference value of fuel cell
 521 efficiency of 65% are 3.5%, 1.7%, and 1.4% compared to the
 522 ECMS, state-based, and the original PI strategies respectively.
 523
 524

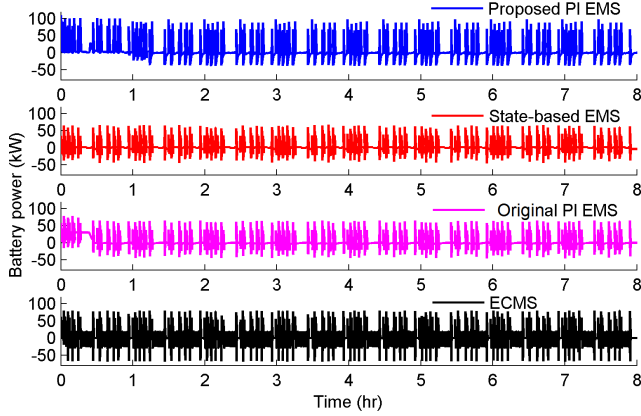


Figure 22: Battery power during the examined voyage using different strategies

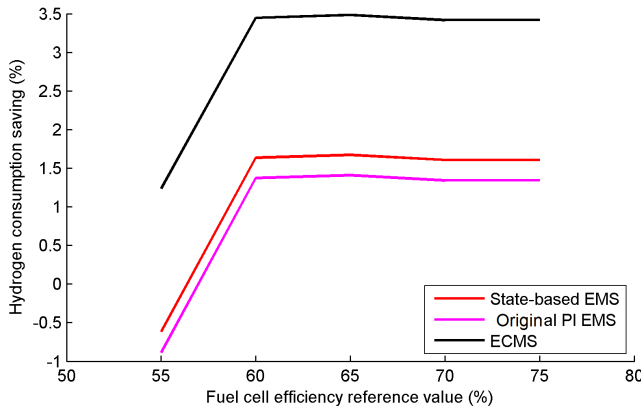


Figure 23: Fuel cell efficiency reference values effect on the hydrogen consumption saving percentage of the proposed PI strategy

4.4.2. Stress analysis

The lifetime of the hybrid fuel cell/battery system, reliability and durability depend mainly on the intended application and the stress on each power source of the hybrid system. Since fuel cells have shorter life and higher maintenance and replacement costs compared to batteries, more focus is now on extending the lifetime of fuel cells [37, 38]. Reducing fuel cell operational stresses can significantly help in extending its lifetime and reducing its fuel consumption. Therefore, it is proposed to take fuel cell efficiency into consideration by the EMS in order to avoid operating the fuel cell away from high efficiency region.

The approach suggested in [9] to determine the stress on the fuel cell and the battery is used in this study. This approach uses Haar wavelet transform to decompose the instantaneous power from the fuel cell and battery into approximation coefficients which contains the low frequency components of the power and detail coefficients which contain the high frequency components [39]. The standard deviation of the high frequency components can give a good indication of the stress on each power source of the hybrid fuel cell/battery system for the examined mission profile. As shown in Table 5, the proposed PI EMS has the low-

est fuel cell stress while it has higher battery stress than other strategies as a result of the trade-off issue between the stresses on the fuel cell and the battery. Moreover, the proposed PI EMS has the lowest hydrogen consumption and more use of the battery energy. An overall performance comparison of the proposed PI EMS is presented in Table 5 using the optimum reference value of the fuel cell efficiency of 65% for the proposed PI EMS as discussed earlier.

4.4.3. Total energy & cost analysis

In order to have a fair comparison between different strategies, the total cost and total consumed energy during the 8 hours period of operation should be calculated and compared. The total cost includes hydrogen cost and the cost of charging the battery back to its initial SOC assuming charging efficiency of 88% [40]. In this study, hydrogen cost is assumed to be 4.823 \$/kg and the battery energy cost is assumed to be 0.284 \$/kWh using shore-shared (or shore-side) energy [41]. The total energy is calculated as a function of the consumed power from the fuel cell from (4) and the battery depleted energy from (7) during the examined voyage.

Figure 24 shows that adopting the proposed PI EMS results in an energy saving of 3.4% compared to the ECMS. However, it consumes more energy than the state-based EMS and the original PI strategies by 3.1% and 2.7% respectively for the examined 8 hours of operation. Moreover, adopting the proposed PI EMS results in a cost saving of 3.3% compared to the ECMS as well but its operating cost is higher than the state-based EMS and the original PI strategies by 10% and 8.7% respectively at the end of the examined 8 hours of operation as shown in Figure 25.

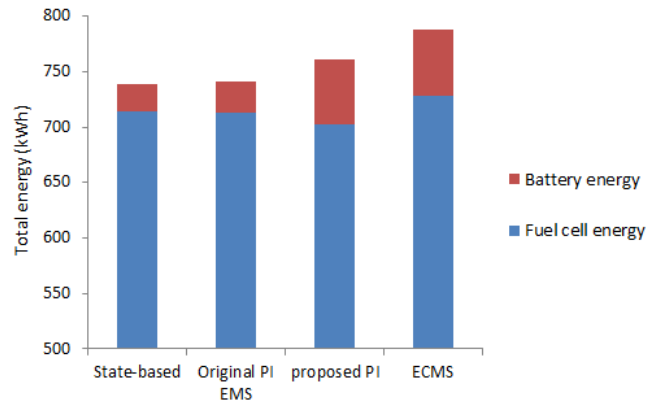


Figure 24: Comparison of total consumed energy during the examined voyage using different strategies

The reported cost saving percentages is calculated according to the assumed prices of hydrogen and electricity however, these prices varies temporally and spatially. Therefore, an energy price ratio (β) is used to study the effect of changing energy price on the operating cost saving,

Table 5: Overall performance comparison

	Proposed PI EMS	State-based EMS	Original PI EMS	ECMS
Fuel cell stress	19.94	29.1	32.29	36.54
Battery stress	32.81	13.03	15.24	26.53
Hydrogen consumption (kg)	17.83	18.13	18.08	18.47
Battery SOC (%)	65 – 59.95	65 – 61.6	65 – 59.97	65 - 64.24

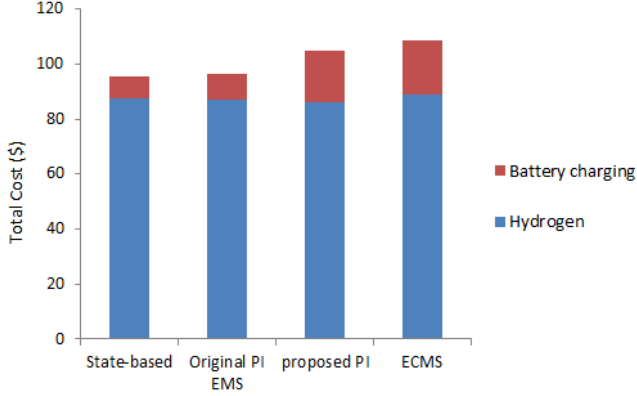


Figure 25: Comparison of total operating cost of the examined voyage using different strategies

586 it can be defines as follows.

$$\beta = \frac{\text{Price of Hydrogen per kWh}}{\text{Price of Electricity per kWh}} \quad (8)$$

587 According to the assumed prices of hydrogen and elec-
588 tricity, $\beta = 0.43$ which corresponds to 4.823 \$/kg of hy-
589 drogen, 39.4 kWh/kg hydrogen energy density, and 0.284
590 \$/kWh of electricity. Different values of β are assumed
591 and its impact on the operating cost saving percentages of
592 adopting the proposed PI EMS compared to state-based,
593 original PI EMS, and ECMS is shown in Figure 26 where
594 higher values of β means that hydrogen becomes more ex-
595 pensive relative to fixed electricity prices.

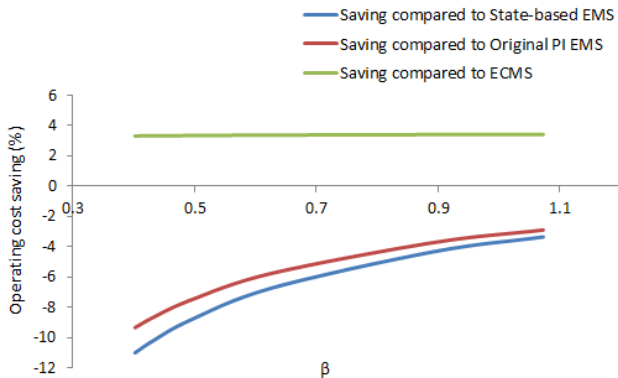


Figure 26: Impact of energy price ratio on operating cost saving percentages of adopting the proposed PI EMS compared to other strategies

596 As can be seen in Figure 26, operating cost saving per-

centages of the proposed PI EMS compared to the state-
597 based EMS and the original PI EMS become higher for
598 higher values of β meanwhile the operating cost saving per-
599 centage of the proposed PI EMS compared to the ECMS
600 doesn't change noticeably for higher values of β . This can
601 be justified by the fact that the state-based and the origi-
602 nal PI strategies tend to use less battery energy therefore
603 it is more affected by changing hydrogen price and β .
604

5. Conclusion

605
606 The design of green ships has generated significant re-
607 cent research interest in order to comply with the more
608 stringent environmental regulations. Without these regu-
609 lations, CO_2 emissions may increase by up to 250% by
610 2050 according to the last IMO study. Therefore, using
611 fuel cells in hybrid electric propulsion systems are attract-
612 ing widespread interest because of its advantages of high
613 efficiency, low emission and quiet operation. The efficiency
614 and performance of fuel cell hybrid systems depend con-
615 siderably on the used energy management strategy which
616 is responsible for splitting the required power between the
617 different components of the hybrid system.

618 In this paper, we first propose an improved PI energy
619 management strategy for marine applications that takes
620 fuel cell efficiency into consideration as an input. The pro-
621 posed strategy has been studied for the first fuel cell pas-
622 senger vessel showing better performance than the state-
623 based strategy developed for the same vessel as well as the
624 original PI and ECMS strategies in terms of hydrogen con-
625 sumption and fuel cell stresses with no additional first cost
626 or hardware changes. For a full driving cycle of 8 hours,
627 a performance comparison has been made in terms of total
628 consumed energy, total cost, battery state of charge,
629 fuel cell efficiency, hydrogen consumption, and the stress
630 seen by each power source. Simulation results show that a
631 daily hydrogen saving of 3.5%, 1.7%, and 1.4% compared
632 to the ECMS, state-based, and the original PI strategies
633 respectively can be achieved by adopting the proposed PI
634 strategy. Also, the proposed strategy has lower energy and
635 operational cost than the ECMS strategy but it has higher
636 energy and operational cost than the state-based and origi-
637 nal PI strategies. Moreover, taking fuel cell efficiency into
638 consideration as an input to the energy management strat-
639 egy as proposed in this study has contributed in better
640 fuel cell performance during operation and less stress on
641 the fuel cell stack which prolongs its lifetime and resulted
642 in less hydrogen consumption.

643 Acknowledgement

644 This research is funded by the Egyptian Government.

645 References

- 646 [1] R. K. Ahluwalia, X. Wang, Fuel cell systems for transportation:
647 status and trends, *Journal of power sources* 177 (2008) 167–176.
- 648 [2] E. K. Dedes, D. A. Hudson, S. R. Turnock, Assessing the po-
649 tential of hybrid energy technology to reduce exhaust emissions
650 from global shipping, *Energy Policy* 40 (2012) 204–218.
- 651 [3] Z. Bazari, T. Longva, Assessment of IMO mandated energy effi-
652 ciency measures for international shipping, *International Mar-
653 itime Organization* (2011).
- 654 [4] M. C. Díaz-de Baldasano, F. J. Mateos, L. R. Núñez-Rivas,
655 T. J. Leo, Conceptual design of offshore platform supply vessel
656 based on hybrid diesel generator-fuel cell power plant, *Applied
657 Energy* 116 (2014) 91–100.
- 658 [5] J. T. Pukrushpan, A. G. Stefanopoulou, H. Peng, Control of
659 fuel cell breathing, *Control Systems, IEEE* 24 (2004) 30–46.
- 660 [6] Y. Wang, K. S. Chen, J. Mishler, S. C. Cho, X. C. Adroher,
661 A review of polymer electrolyte membrane fuel cells: technol-
662 ogy, applications, and needs on fundamental research, *Applied
663 Energy* 88 (2011) 981–1007.
- 664 [7] J. Torreglosa, P. Garcia, L. Fernandez, F. Jurado, Predictive
665 control for the energy management of a fuel-cell–battery–su-
666 percapacitor tramway, *IEEE Transactions on Industrial Informa-
667 tics* 10 (2014) 276–285.
- 668 [8] L. Xu, M. Ouyang, J. Li, F. Yang, L. Lu, J. Hua, Optimal
669 sizing of plug-in fuel cell electric vehicles using models of vehicle
670 performance and system cost, *Applied Energy* 103 (2013) 477–
671 487.
- 672 [9] S. N. Motapon, L.-A. Dessaint, K. Al-Haddad, A compara-
673 tive study of energy management schemes for a fuel-cell hybrid
674 emergency power system of more-electric aircraft, *IEEE Trans-
675 actions on Industrial Electronics* 61 (2014) 1320–1334.
- 676 [10] A. Fadel, B. Zhou, Power management methodologies for fuel
677 cell-battery hybrid vehicles, *Technical Report, SAE Technical
678 Paper*, 2010.
- 679 [11] L. Xu, M. Ouyang, J. Li, F. Yang, L. Lu, J. Hua, Application of
680 pontryagin’s minimal principle to the energy management strat-
681 egy of plugin fuel cell electric vehicles, *International Journal of
682 Hydrogen Energy* 38 (2013) 10104 – 10115.
- 683 [12] Q. Cai, D. Brett, D. Browning, N. Brandon, A sizing-design
684 methodology for hybrid fuel cell power systems and its appli-
685 cation to an unmanned underwater vehicle, *Journal of Power
686 Sources* 195 (2010) 6559–6569.
- 687 [13] I. Valero, S. Bacha, E. Rulliere, Comparison of energy manage-
688 ment controls for fuel cell applications, *Journal of power sources*
689 156 (2006) 50–56.
- 690 [14] P. Thounthong, S. Ral, B. Davat, Energy management of fuel
691 cell/battery/supercapacitor hybrid power source for vehicle ap-
692 plications, *Journal of Power Sources* 193 (2009) 376 – 385.
- 693 [15] J. Han, J.-F. Charpentier, T. Tang, An energy management
694 system of a fuel cell/battery hybrid boat, *Energies* 7 (2014)
695 2799–2820.
- 696 [16] L. Zhu, J. Han, D. Peng, T. Wang, T. Tang, J.-F. Charpen-
697 tier, Fuzzy logic based energy management strategy for a fuel
698 cell/battery/ultra-capacitor hybrid ship, in: *International Con-
699 ference on Green Energy, IEEE*, 2014, pp. 107–112.
- 700 [17] C. H. Choi, S. Yu, I.-S. Han, B.-K. Kho, D.-G. Kang, H. Y. Lee,
701 M.-S. Seo, J.-W. Kong, G. Kim, J.-W. Ahn, S.-K. Park, D.-W.
702 Jang, J. H. Lee, M. Kim, Development and demonstration of
703 PEM fuel-cell-battery hybrid system for propulsion of tourist
704 boat, *International Journal of Hydrogen Energy* 41 (2016) 3591
705 – 3599.
- 706 [18] N.-C. Shih, B.-J. Weng, J.-Y. Lee, Y.-C. Hsiao, Development of
707 a 20 kw generic hybrid fuel cell power system for small ships and
708 underwater vehicles, *International Journal of Hydrogen Energy*
709 39 (2014) 13894–13901.
- [19] C. Thimm, Zemsips - the first fuel cell passenger ship in ham- 710
burg, in: *ZERO REGIO Workshop, Montecatini Terme, Italy,* 711
2007. 712
- [20] J. J. de Troya, C. Ivarez, C. Fernandez-Garrido, L. Carral, 713
Analysing the possibilities of using fuel cells in ships, *Inter-
714 national Journal of Hydrogen Energy* 41 (2016) 2853 – 2866. 715
- [21] HADAG, [http://www.hadag.de/english/harbour-ferries.](http://www.hadag.de/english/harbour-ferries.html) 716
[html](http://www.hadag.de/english/harbour-ferries.html), 2015. Accessed: 2015-09-04. 717
- [22] S. F. Tie, C. W. Tan, A review of energy sources and energy 718
management system in electric vehicles, *Renewable and Sus-
719 tainable Energy Reviews* 20 (2013) 82 – 102. 720
- [23] P. Garcia, L. M. Fernandez, C. A. Garcia, F. Jurado, Energy 721
management system of fuel-cell-battery hybrid tramway, *Indus-
722 trial Electronics, IEEE Transactions on* 57 (2010) 4013–4023. 723
- [24] W. Choi, J. Howze, P. Enjeti, Development of an equivalent 724
circuit model of a fuel cell to evaluate the effects of inverter
725 ripple current, *Journal of Power Sources* 158 (2006) 1324 –
726 1332. 727
- [25] MATLAB control system toolbox, [http://uk.mathworks.com/
728 products/control/](http://uk.mathworks.com/products/control/), 2016. Accessed: 2016-07-18. 729
- [26] L. Xu, J. Li, J. Hua, X. Li, M. Ouyang, Optimal vehicle control 730
strategy of a fuel cell/battery hybrid city bus, *International
731 Journal of Hydrogen Energy* 34 (2009) 7323 – 7333. 732
- [27] G. Paganelli, S. Delprat, T. M. Guerra, J. Rimaux, J. J. Santin, 733
Equivalent consumption minimization strategy for parallel hybrid
734 powertrains, in: *Vehicle Technology Conference, 2002.*
735 *VTC Spring 2002. IEEE 55th, volume 4, 2002, pp. 2076–2081*
736 *vol.4. doi:10.1109/VTC.2002.1002989.* 737
- [28] L. Xu, J. Li, J. Hua, X. Li, M. Ouyang, Adaptive supervisory 738
control strategy of a fuel cell/battery-powered city bus, *Journal
739 of Power Sources* 194 (2009) 360–368. 740
- [29] S. Njoya, O. Tremblay, L.-A. Dessaint, A generic fuel cell model 741
for the simulation of fuel cell vehicles, in: *Vehicle Power and
742 Propulsion Conference, 2009. VPPC’09. IEEE, IEEE, 2009, pp.*
743 *1722–1729.* 744
- [30] Mathworks, <http://uk.mathworks.com/help/>, 2015. Accessed: 745
2015-08-30. 746
- [31] L. Barelli, G. Bidini, A. Ottaviano, Optimization of a 747
PEMFC/battery pack power system for a bus application, *Ap-
748 plied energy* 97 (2012) 777–784. 749
- [32] *Fuel Cell Handbook (Seventh Edition)*, Technical Report, EG 750
& G Technical Services, Inc., 2004. Contract No.DE-AM26-
751 99FT40575. 752
- [33] O. Tremblay, L.-A. Dessaint, Experimental validation of a bat- 753
tery dynamic model for EV applications, *World Electric Vehicle
754 Journal* 3 (2009) 1–10. 755
- [34] M. Ouyang, L. Xu, J. Li, L. Lu, D. Gao, Q. Xie, Performance 756
comparison of two fuel cell hybrid buses with different pow-
757 ertrain and energy management strategies, *Journal of Power
758 Sources* 163 (2006) 467–479. 759
- [35] P. Garcia, J. Torreglosa, L. Fernandez, F. Jurado, Viability study 760
of a fc-battery-sc tramway controlled by equivalent consump-
761 tion minimization strategy, *International Journal of Hydrogen
762 Energy* 37 (2012) 9368 – 9382. 763
- [36] D. Tilman, C. L. Lehman, C. E. Bristow, Diversity-stability re- 764
lationships: statistical inevitability or ecological consequence?,
765 *The American Naturalist* 151 (1998) 277–282. 766
- [37] C.-H. Chao, J.-J. Shieh, A new control strategy for hybrid fuel 767
cell-battery power systems with improved efficiency, *Internat-
768 ional Journal of Hydrogen Energy* 37 (2012) 13141 – 13146. 769
- [38] J. Zhuo, C. Chakrabarti, K. Lee, N. Chang, S. Vrudhula, Max- 770
imizing the lifetime of embedded systems powered by fuel cell-
771 battery hybrids, *IEEE Transactions on Very Large Scale Integ-
772 ration (VLSI) Systems* 17 (2009) 22–32. 773
- [39] S. Lahmiri, Wavelet low- and high-frequency components as 774
features for predicting stock prices with backpropagation neural
775 networks, *Journal of King Saud University - Computer and
776 Information Sciences* 26 (2014) 218 – 227. 777
- [40] A. Foley, B. Tyther, P. Calnan, B. Gallachir, Impacts of elec- 778
tric vehicle charging under electricity market operations, *Ap-* 779
plied Energy 163 (2016) 100–110. 780

781 plied Energy 101 (2013) 93 – 102. Sustainable Development of
782 Energy, Water and Environment Systems.
783 [41] R. Winkel, U. Weddige, D. Johnsen, V. Hoen, G. Pa-
784 paefthymiou, Potential for Shore Side Electricity in Europe,
785 Technical Report, ECOFYS Consultancy, 2015. Project num-
786 ber:TRANL14441.